APPROPRIATE MODELS FOR PRACTICAL NONLINEAR DYNAMIC ANALYSIS OF REINFORCED CONCRETE FRAMES

A. Lepage[1], S. A. Delgado[1], and J. J. Dragovich[2]

[1]Department.of Architectural Engineering, The Pennsylvania State University, University Park, PA, USA
[2]Department of Civil and Environmental Engineering, Seattle University, Seattle, WA, USA
Email: lepage@psu.edu, sadelgado@gmail.com, jeffdrag@seattleu.edu

ABSTRACT:
The object of this paper is to identify the optimal combination of hysteresis-model and damping parameters that lead to the best correlation between the calculated and measured seismic response. The combined effects of five parameters are investigated: initial stiffness, bond-slip deformations, post-yield stiffness, unloading stiffness, and type of damping. The first four of these parameters are implemented using the Takeda hysteresis model to characterize the moment-rotation dynamic response of individual frame members. The analyses use lumped-plasticity models concentrated at member ends. The study uses the recorded seismic responses of two ten-story laboratory structures and two orthogonal structural systems in an existing seven-story building. For each case of analysis, the calculated roof displacement history is compared to the measured response by means of the frequency domain error index (*FDE*), facilitating the identification of the combination of parameters that leads to the best analytical simulation. Although the best simulations are attained in models with uncracked initial stiffness, hard post-yield stiffness, and reducing unloading stiffness, models with cracked initial stiffness that lead to satisfactory simulations are also identified.

KEYWORDS: Frequency-domain error, time-history analysis, calculated vs. measured.

1. INTRODUCTION

In the seismic evaluation of existing buildings as well as in the design of new ones, there are situations where a third-party review is required for obtaining a building permit. It is current practice for designers to proportion new buildings with seemingly subtle deviations from the building codes. Moment redistribution, effective section properties, effective damping, beam-column joint strength, member dimensions, etc. are some of the items designers often choose to treat with an unconventional perspective. These deviations end up triggering a peer review. Not surprisingly, the reviewers often mandate the use of advanced seismic analyses based on nonlinear static or dynamic procedures. In addition, design engineers are increasingly using nonlinear analyses to evaluate the relative merits of different framing configurations and/or proportioning schemes.

The main objective of this study is to identify a set of modeling parameters that lead to reliable simulations when performing nonlinear dynamic analysis. The study uses measured response data for two ten-story experimental structures (MF1, MF2) tested in the University of Illinois earthquake simulator, and for the two orthogonal structures (HEW, HNS) of the seven-story Holiday Inn building (Van Nuys, Calif.) recorded during the 1994 Northridge earthquake. For each of the four structures, five basic modeling parameters are considered: initial stiffness, bond-slip deformations, post-yield stiffness, unloading stiffness, and type of damping.

2. NONLINEAR DYNAMIC ANALYSIS

A variant of program LARZ[1] was used for the nonlinear dynamic analysis. Most of the built-in assumptions in LARZ may be easily implemented in other commercially available programs. In a section below, results are presented for nonlinear dynamic analyses using programs SAP2000 and PERFORM3D (www.csiberkeley.com). Program LARZ considers beams and columns as massless line elements with a linearly-elastic middle portion bounded by nonlinear rotational springs. The springs connect to rigid finite segments representing the beam-column joint. Axial deformations are neglected and therefore beams are part of a rigid diaphragm and vertical column displacements are not considered. Stiffness characteristics of the structure remain unchanged over short time increments but are redefined at the end of each time interval. Masses are lumped at floor levels where the horizontal degrees of freedom are defined. P-Δ effects are taken into account.

For each element, moment-rotation relationships due to flexure are derived using user-defined trilinear moment-curvature relationships of unbounded ductility with breakpoints at cracking and yielding. The moment-rotation

primary curves account for bond-slip assumed to occur at beam-column joints. Shear stiffness is taken into account and assumed constant. The damping matrix, [*C*], is constructed by linear combination of the mass [*M*] and stiffness [*K*] matrix, both defined at global structural degrees of freedom (Rayleigh damping):

$$[C] = \alpha [M] + \beta [K] \quad (1)$$

$$\xi_i = \frac{1}{2\omega_i}\left(\alpha + \beta \omega_i^{\,2}\right) \quad (2)$$

where ξ_i is the fraction of critical damping for mode *i* of frequency ω_i. In this study, damping is defined as a function of the first-mode frequency, ω_1, based on uncracked section properties. For the case of mass proportional damping, $\alpha=2\xi_1\omega_1$ and $\beta=0$, where α affects the unchanging [*M*] matrix. For stiffness-proportional damping, $\alpha=0$ and $\beta=2\xi_1/\omega_1$, where β affects the continuously updated [*K*] matrix.

2. TEST STRUCTURES MF1 and MF2

Structure MF1 tested by Healey[2] and structure MF2 tested by Moehle[3], comprised two 10-story frames working in parallel. The first and tenth stories for both frames in structure MF1 were taller than the others as shown in Fig. 1. Frames in test structure MF2 had identical geometry to MF1 except for the discontinued beams at one bay of the first story. Cross-sectional dimensions for both test structures were the same. Story weights were nominally 4.45 kN, with the exception of the first story in model MF2, where nearly 2/3 of the weight was used. The weights were transferred directly to the column centerlines such that each column carried equal fraction of the story weight (except for the first floor of MF2). The specimens were fixed at their base to heavy girders which were bolted to the test platform of the University of Illinois earthquake simulator. The base motions were patterned after El Centro 1940 NS, normalized to 0.40g for MF1 and 0.38g for MF2, with a time scale compressed by a factor of 2.5 to obtain realistic ratios between the input frequency contents and natural frequencies of the small-scale specimens.

Both specimens were cast using small-aggregate concrete with compressive strength, f'_c, of 40 MPa in MF1 and 38 MPa in MF2. Concrete modulus of elasticity was approximately 22,000 MPa. Axial load in the first-story columns did not exceed 0.2 $f'_c\ A_g$. All members were reinforced by steel wire gage No. 13 and 16, longitudinally and transversely, respectively. Longitudinal reinforcement was continuous through all joints and extended into exterior joint stubs for anchorage. Transverse reinforcement provided by rectangular spirals prevented shear failure before flexural failure. Beam-column joints were reinforced with helical spirals to prevent joint failures. More details are found in Healey[2] and Moehle[3].

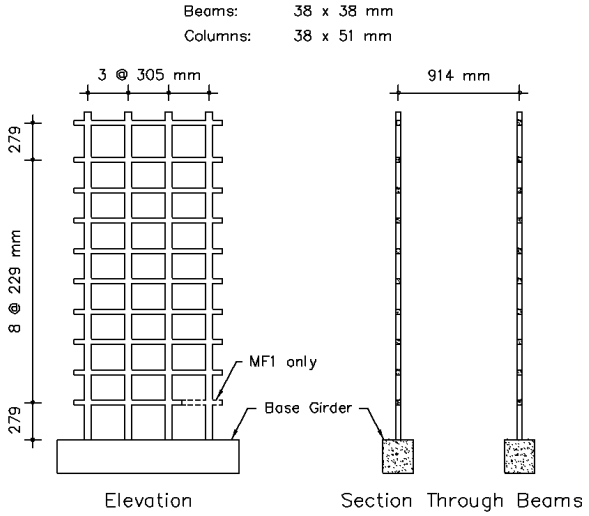

Fig. 1 Test Structures MF1 and MF2

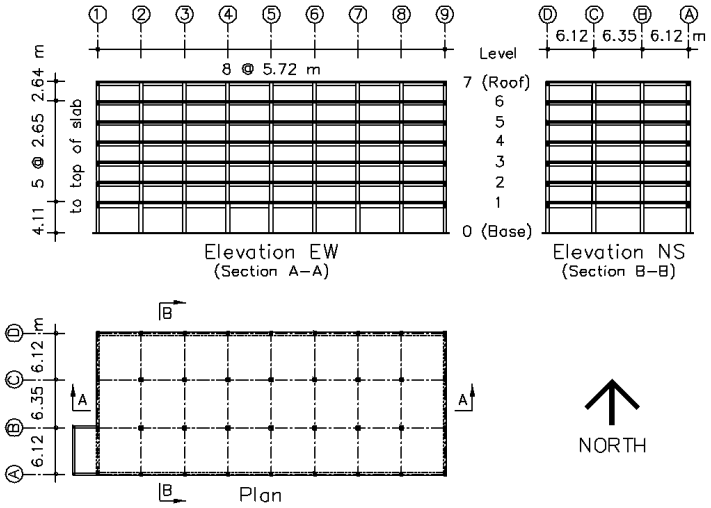

Fig. 2 Holiday Inn Building, Van Nuys, California.

3. HOLIDAY-INN BUILDING AT VAN NUYS, CALIFORNIA

The seven-story reinforced concrete hotel building was built in 1966 on the northeast side of Los Angeles basin at ±6 km from the epicenter of the 1994 Northridge earthquake[4]. The structure is essentially symmetrical in plan about both axes. Light framing members support the stairway and elevator openings located on the southwest end (Fig. 2). All concrete is normal-weight with the first-story columns having a minimum specified compressive strength of 34 MPa. The first-level floor slab and columns between levels 1 and 2 were built with 28-MPa concrete, all other concrete above grade had a specified concrete strength of 21 MPa. Columns used ASTM-A432 steel with specified yield of 410 MPa, while beams and slabs used 280-MPa steel.

Seismic design was based on the assumption that the code-specified lateral forces were resisted by the combined action of the interior slab-column frames and exterior beam-column frames. The interior columns are 510-mm square in the first story and 460-mm square above. Exterior columns are 360x510 mm for full building height. Column transverse reinforcement spaced at 300 mm is noncompliant with modern special moment frame requirements.

The structure damage due to the 1994 Northridge earthquake was serious. The perimeter frames had extensive cracking of concrete related to shear and bond stresses, especially at columns. A total of 16 accelerometers located at the roof, fifth, second, first, and ground levels recorded motions in the EW, NS, and vertical directions. The recorded peak ground acceleration was 0.45g and 0.42g in the EW and NS directions.

4. PARAMETERS OF ANALYSIS

The influence of five basic modeling parameters required for nonlinear dynamic analysis is considered:

4.1 Initial Stiffness

The initial slope of the moment-curvature relationships are determined assuming member sections are either uncracked (U) or cracked (C). For U cases, the initial stiffness is defined based on gross section properties and the cracking point is defined based on a modulus of rupture of $\frac{5}{8}\sqrt{f'_c}$ [MPa]. For C cases, the initial stiffness is defined using the secant stiffness to the yield point calculated based on perfect-bond between concrete and steel. Concrete stress-strain variation was based on the model by Hognestad[5].

4.2 Bond-Slip Deformations

The primary moment-rotation curves are determined from moment-curvature relationships assuming a midspan inflection point. These primary curves are modified by adding the rotation due to bond slip, θ', occurring at beam-column joints for an average bond stress, u:

$$\theta' = \frac{1}{8}\frac{d_b f_y^2}{E_s u (d-d')}\left(\frac{M}{M_y}\right)^2 \qquad (3)$$

where, d_b is the diameter of the steel bar in tension, E_s the steel modulus, f_y the steel yield stress, d and d' define the steel locations, and M_y is the yield moment.

Two cases are considered, Tight (T) where u is taken as $\frac{2}{3}\sqrt{f'_c}$ [MPa], and Loose (L) where u is taken as $\frac{1}{3}\sqrt{f'_c}$ [MPa]. Values of θ' are obtained for the cracking moment and yield moment. The parameter θ' for other values of $M \le M_y$ is linearly interpolated. Although beam-column joints are assumed rigid, the values of θ' that correspond to L cases may also be interpreted as joints having a non-rigid portion.

4.3 Post-Yield Stiffness

The moment-rotation post-yield stiffness, K_p, is expressed as a fraction of the secant stiffness to yield, K_e. The yield point is defined after consideration of bond-slip effects. Two cases are considered: a Soft (S) case where $K_p = 0.02\ K_e$ and a Hard (H) case where $K_p = 0.10\ K_e$. To ensure the target post-yield stiffness, modifications to LARZ[1] were implemented.

4.4 Unloading Stiffness

Hysteresis rules are based on the model by Takeda[6]. The unloading slope of the moment-rotation hysteresis model is controlled by the exponent γ:

$$K_r = K_e\left(\frac{\theta_e}{\theta_m}\right)^{\gamma} \qquad (4)$$

where K_r is the unloading stiffness, K_e the secant stiffness to the yield point, θ_e the yield rotation, and θ_m the maximum rotation attained. Two values of γ are considered: zero to represent a Non-reducing (N) unloading slope and 0.5 to represent a Reducing (R) case.

4.5 Viscous Damping

Four cases for the amount and type of damping are considered: mass proportional damping at 2% and 5% of critical, and stiffness proportional at 2% and 5% of critical, identified as α_2, α_5, β_2, β_5. The constants α and β (Eq. 1) are based on the first mode of vibration and computed using uncracked section properties (even for C cases).
Table 1 presents a summary of the five modeling parameters considered. Four parameters adopt two values and a fifth parameter adopts four values, giving 64 combinations for each structure (MF1, MF2, HEW, HNS).
For structures MF1 and MF2, material properties were obtained from standard laboratory procedures. For structures HEW and HNS, material strengths were taken as 1.1 times the specified strength.

Table 1 Parameter Identification

Parameter			Symbol
Initial Stiffness:	Uncracked	($f_r = \frac{5}{6}\sqrt{f'_c}$) [MPa]	U
	Cracked	($f_r \sim 0$)	C
Bond-Slip:	Tight	($u = \frac{2}{3}\sqrt{f'_c}$) [MPa]	T
	Loose	($u = \frac{1}{3}\sqrt{f'_c}$)	L
Post-Yield Stiffness:	Hard	(K_p = 0.10 Ke)	H
	Soft	(K_p = 0.02 Ke)	S
Unloading Stiffness:	Non Reducing	(γ = 0)	N
	Reducing	(γ = 0.5)	R
Viscous Damping:	2% Mass Proportional		α_2
	5% Mass Proportional		α_5
	2% Stiffness Proportional		β_2
	5% Stiffness Proportional		β_5

5. *FDE* INDEX

The large number of models and response data make it impractical to visually discern the set of parameters that give the best correlation between the measured and calculated response for each of the four structures considered. The Frequency Domain Error Index (*FDE*)[7] provides a measure of the correlation between two waveforms. The index is used in this study to identify the models that lead to the best correlations between measured and calculated roof displacements.
The *FDE* index is based on the characteristics of the frequencies contained in the signals under comparison. The index calculation quantifies amplitude and phase deviations between two signals and gives a value between 0 and 1, where 0 indicates a perfect correlation, and 1 indicates a signal 180 degrees out-of-phase.
To determine the *FDE* index, it is necessary to compute the Fourier Transform of both the measured and calculated signals. The signals are then represented as complex numbers in the frequency domain. For each frequency, the real and imaginary components of the complex number can be thought of as x-y coordinates, where the x-axis represents the real component, and the y-axis the imaginary component (Argand diagram). Fig. 3 shows this x-y representation at a specific frequency for the measured and calculated signals.
The *FDE* index is based on the error vector (Fig. 3) normalized by the sum of the vector magnitudes of the measured and calculated signals:

$$FDE = \frac{\sum_{i=f_1}^{f_2} \sqrt{\left(R_{M_i} - R_{C_i}\right)^2 + \left(I_{M_i} - I_{C_i}\right)^2}}{\sum_{i=f_1}^{f_2} \left(\sqrt{R_{M_i}{}^2 + I_{M_i}{}^2}\right) + \left(\sqrt{R_{C_i}{}^2 + I_{C_i}{}^2}\right)} \qquad (5)$$

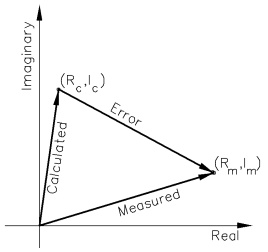

Fig. 3 *FDE* Representation

where, R_{M_i}, I_{M_i} = real and imaginary component of the measured signal at frequency i
R_{C_i}, I_{C_i} = real and imaginary component of the calculated signal at frequency i
f_1, f_2 = starting and ending frequency for summation.

The denominator in Eq. 5 normalizes the frequency domain error to values between 0 and 1. For this study, frequencies f_1 and f_2 are defined as a function of the fundamental period, T_1, of the uncracked structure, using $1/(4T_1)$ and $1/(0.1T_1)$, respectively. This range is expected to capture the most relevant frequency content of the signals representing inelastic structural response.

6. DISCUSSION OF RESULTS

The roof displacement is capable of characterizing global and local responses with reasonable accuracy in regular frame structures[1]. In this study, to evaluate the goodness of fit of the calculated responses, the roof displacement signal was chosen as the key response parameter.

The calculated displacement response is compared to the measured response by means of the *FDE* index. Results are presented in the *FDE* index charts (Fig. 4 and 5) consisting of a graphical representation resembling a dart board, where the center of the chart indicates a *FDE* of zero or a perfect correlation between the measured and calculated response histories. A point near the periphery (*FDE* = 0.75) represents a very poor correlation. The circle is divided into 16 sectors, with each sector representing one of the 16 models derived from the combination of parameters U/C, H/S, N/R, and T/L. Charts are presented for structures MF1 and MF2 (Fig. 4) and structures HEW and HNS (Fig. 5) with a separate plot for each value of damping assumed (α_2, α_5, β_2, β_5).

In Fig. 4 and 5 the right half of each circle refers to U models and the left half refers to C models. The first sector of the first quadrant marks the model most resistant to deformation, model UHNT, and the model with opposite properties, located at 180°, marks the model least resistant to deformation, model CSRL. Every sector, identifying a given model, has an opposite sector identifying the model with the alternative parameter values. Each data point in Fig. 4 and 5 represent not only the *FDE* indexes, but may also show a cross identifying the cases where the amplitude of the maximum calculated displacement differs from the maximum measured displacement by more than 25%.

To identify the best models, the *FDE* index data were sorted for each type of structure and damping. For U models applied to all four structures, only two parameter combinations had both a *FDE* index less than or equal to 0.25 and maximum calculated displacements within 25% of the maximum measured. These models are UHRL-β_5 and UHRT-β_2, with an average *FDE* index of 0.20 and 0.21, respectively. The average *FDE* is calculated using data for the four structures considered. The roof displacement histories for models UHRT-β_5 are shown in Fig. 6 exhibiting satisfactory correlations.

For C models, only two parameter combinations had both a *FDE* index less than or equal to 0.30 and maximum calculated displacements within 25% of the maximum measured, for all four structures. These models are CHRT-α_2 and CHRL-α_5, with an average *FDE* index of 0.24 and 0.27, respectively. The roof displacement histories for models CHRT-α_2 are shown in Fig. 7 exhibiting satisfactory correlations.

The models also gave satisfactory correlations for base-shear histories as shown in Fig. 8 for UHRL-β_5.

Pilot runs with two other programs, SAP2000 and PERFORM3D (www.csiberkeley.com) were made for C models of the same four structures (MF1, MF2, HEW, and HNS), but at this stage only for damping type α_2. Models built with programs SAP2000 and PERFORM3D using frame line elements, are not currently suitable for U models since moment-rotation characterizations for this element type do not allow breakpoints before the yield point. In SAP2000 the pivot hysteresis model[8] was used and in PERFORM3D the energy dissipation index described by Otani[9] was used to control the hysteresis loops. A summary of the preliminary results are shown in Fig. 9 and 10, where the best *FDE* index averages for C models are also attained by CHRT-α_2 models.

7. CONCLUSIONS

(1) This paper introduces the frequency domain error (*FDE*) index charts as an effective tool for visualizing the influence of multiple parameter values on the correlation between the calculated nonlinear dynamic response and the measured response. The charts help identify the analytical models having the best and most consistent correlation with measured response.

(2) The calculated roof displacement response using uncracked initial stiffness (U models) resulted in lower *FDE* indexes compared to models using cracked initial stiffness (C models).

(3) The following rules consistently led to the lowest *FDE* indexes:

a) use 10% post-yield stiffness ratio and an unloading stiffness parameter γ of 0.5 (i.e. use models with HR);

b) for models using uncracked initial stiffness select stiffness-proportional damping and for models using cracked initial stiffness select mass-proportional damping (i.e., use U models with β, or C models with α);

c) for models where bond-slip is based on a bond stress of $\frac{2}{3}\sqrt{f'_c}$ [MPa] use 2% damping ratio and for a bond stress of $\frac{1}{3}\sqrt{f'_c}$ [MPa] use 5% damping (i.e., use T models with 2% damping or L models with 5% damping)

Thus, for a given damping type the following models outperformed their peers (see Table 1 for parameter Id.): UHRT-β_2, UHRL-β_5, CHRT-α_2, and CHRL-α_5.

(4) When comparing programs LARZ, SAP2000, and PERFORM3D using cracked initial stiffness (C models), the *FDE* index charts indicate that for each program the model with the lowest *FDE* index average is CHRT-α_2.

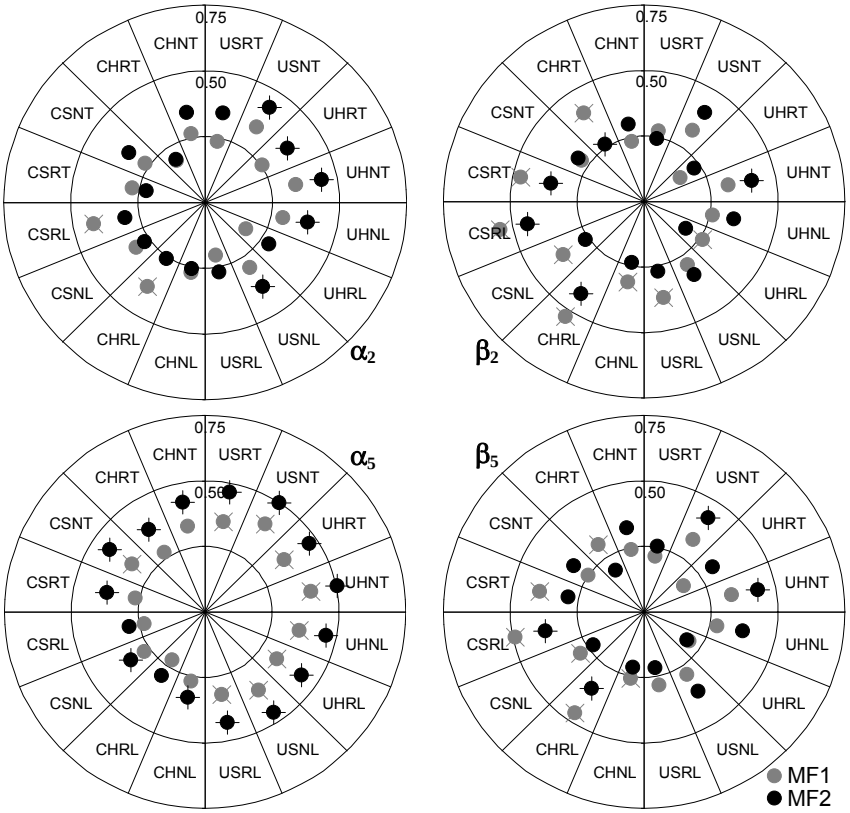

Fig. 4 *FDE* Index Charts, Structures MF1 and MF2, LARZ.

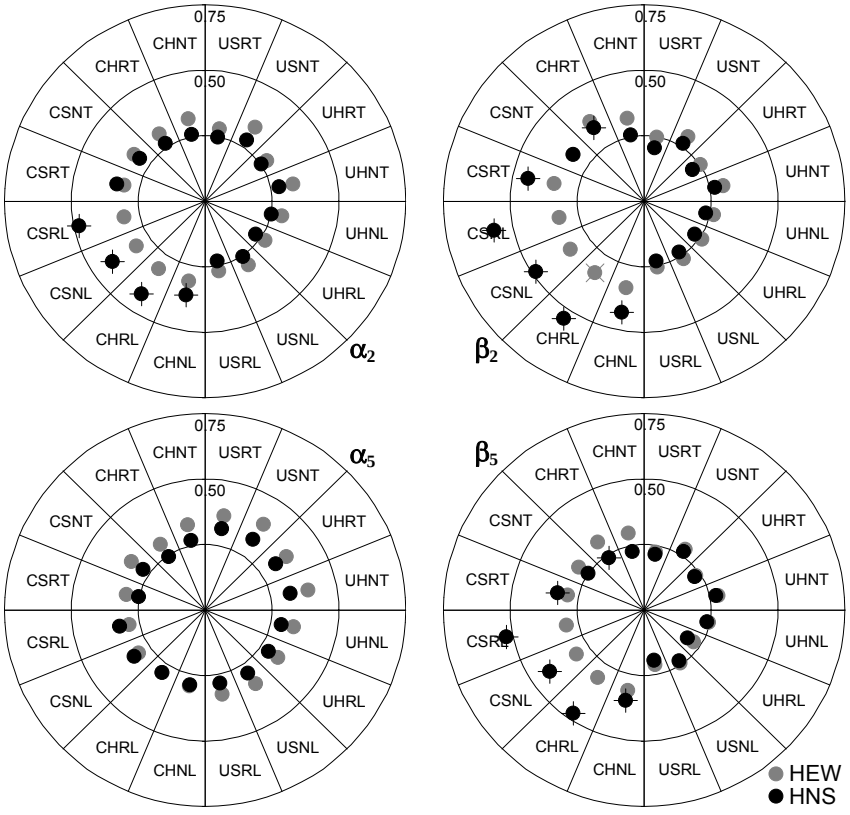

Fig. 5 *FDE* Index Charts, Structures HEW and HNS, LARZ.

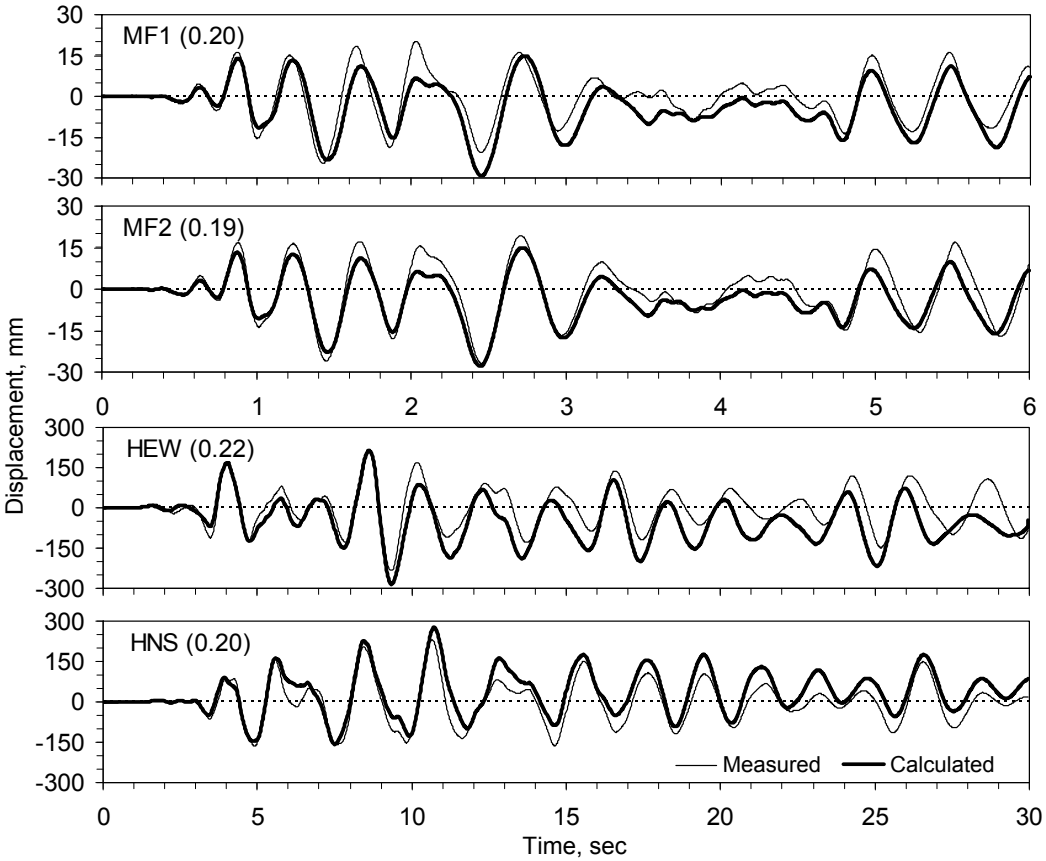

Fig. 6 Displacement Histories, Model UHRL-β_5.

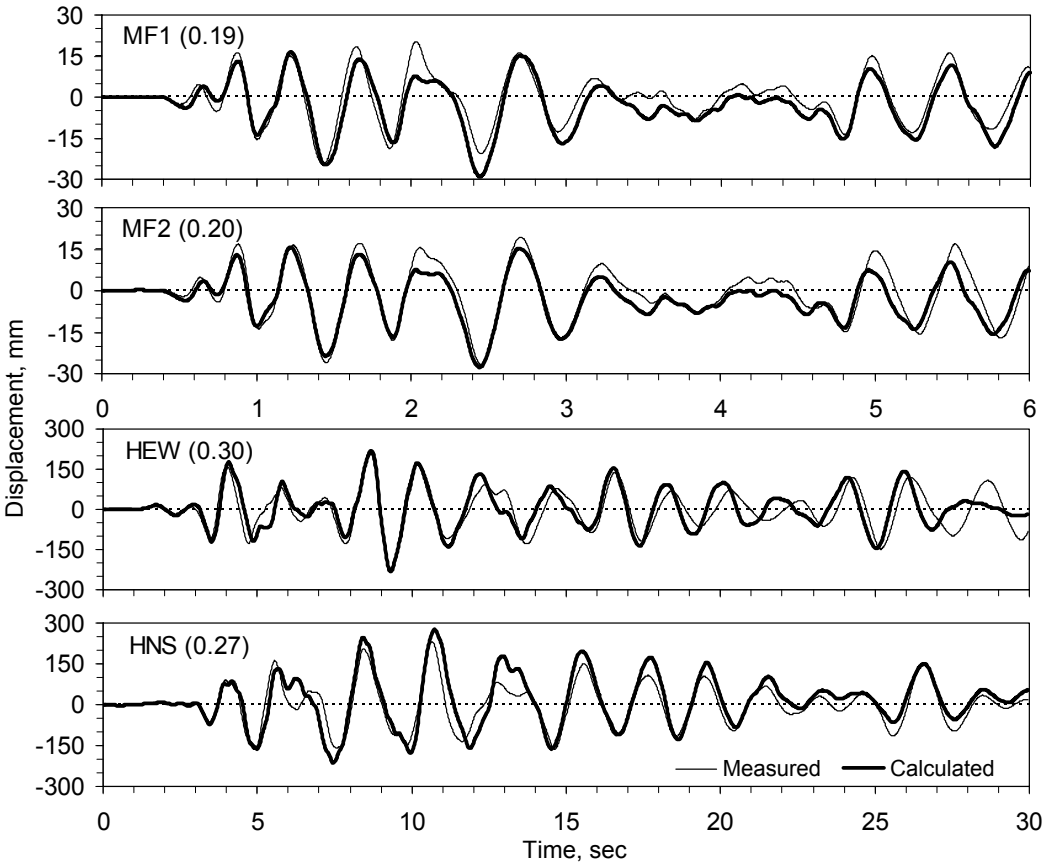

Fig. 7 Displacement Histories, Model CHRT-α_2.

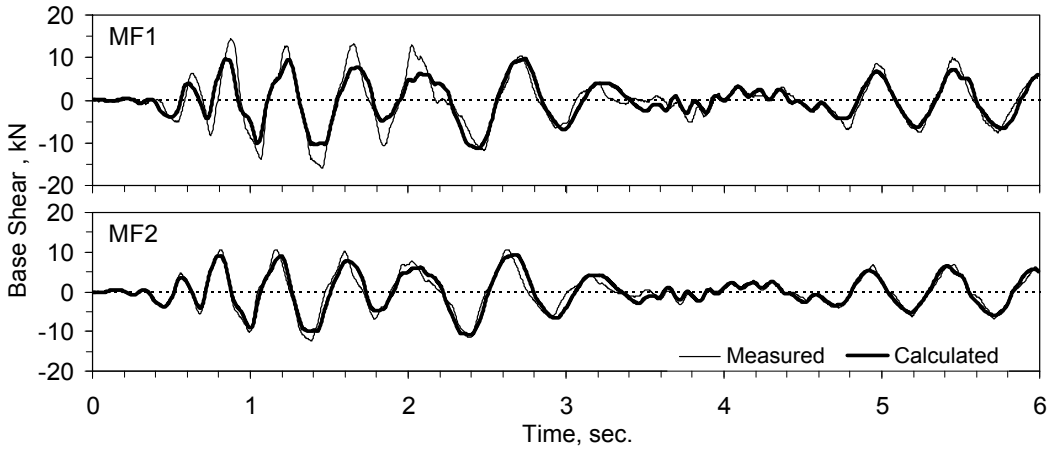

Fig. 8 Base Shear Histories, Model UHRL-β_5.

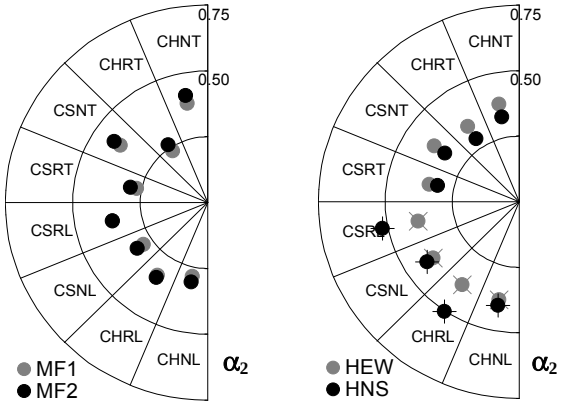

Fig. 9 *FDE* Index Charts, SAP2000

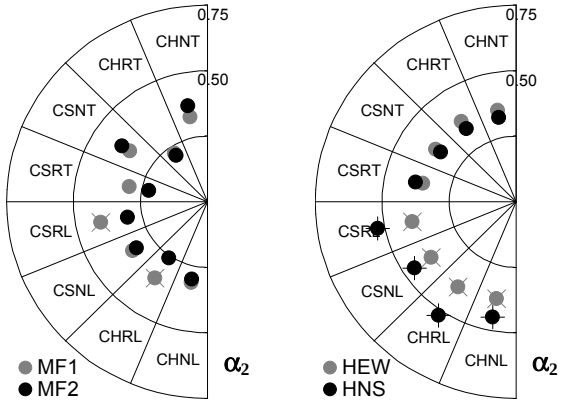

Fig. 10 *FDE* Index Charts, PERFORM3D

ACKNOWLEDGMENTS

The writers are grateful to Mete Sozen (Purdue University) for sharing the data from the University of Illinois earthquake simulator.

REFERENCES

[1] Saiidi, M. and Sozen M. A. (1979). Simple and Complex Models for Nonlinear Seismic Response of Reinforced Concrete Structures, *Structural Research Series*, No. 465, Civil Engineering Studies, University of Illinois, Urbana-Champaign, 188 p.

[2] Healey, T. J. and Sozen M. A. (1978). Experimental Study of the Dynamic Response of a Ten-Story Reinforced Concrete Frame with a Tall First Story, *Structural Research Series*, No. 450, Civil Engineering Studies, University of Illinois, Urbana-Champaign, 120 p.

[3] Moehle, J. P. and Sozen M. A. (1978). Earthquake-Simulation Tests of a Ten-Story Reinforced Concrete Frame with a Discontinued First-Level Beam, *Structural Research Series*, No. 451, Civil Engineering Studies, University of Illinois, Urbana-Champaign, 162 p.

[4] Browning, J. and Lepage, A. (1999). "Discussion of Nonlinear Analyses of an Instrumented Structure Damaged in the 1994 Northridge Earthquake (by Li, Y. and Jirsa, J. O.)", *Earthquake Spectra*, **15:1**, 175-179.

[5] Hognestad, E. (1951). A Study of Combined Bending and Axial Load in Reinforced Concrete Members, *Bulletin Series* No. 399, University of Illinois, Engineering Experiment Station, Urbana-Champaign, 128 p.

[6] Takeda, T., Sozen, M. A., and Nielsen, N. N. (1970). Reinforced Concrete Response to Simulated Earthquakes, *Journal of the Structural Division*, ASCE, **96:ST12**, 2557-2573.

[7] Dragovich, J. (1996). An Experimental Study of Torsional Response of Reinforced Concrete Structures to Earthquake Excitation, Ph.D. Thesis Submitted to the Graduate College of the University of Illinois, Urbana-Champaign, 623 p.

[8] Dowell, R. K., Seible, F., and Wilson, E. L. (1998). Pivot Hysteresis Model for Reinforced Concrete Members, *ACI Structural Journal*, **95:5**, 607-617.

[9] Otani, S. (1981). Hysteresis Models of Reinforced Concrete for Earthquake Response Analysis. Journal of the Faculty of Engineering, University of Tokyo, **36:2**, 125-159.